ATOMIC DATA AND NUCLEAR DATA TABLES **64,** 301–319 (1996)
ARTICLE NO. 0025

ELECTRON–ION COLLISIONAL IONIZATION CROSS SECTIONS FOR THE Li ISOELECTRONIC SEQUENCE

C. CHEN, W. HU, D. FANG, Y. WANG, and F. YANG

T. D. Lee Physics Laboratory, Nuclear-Science Department
Fudan University, Shanghai 200433, China

and

H. TENG

Shanghai Institute of Optical and Fine Mechanics
Academia Sinica, Shanghai 201800, China

In this work, we calculate the electron impact ionization cross sections for Li-like isoelectronic-sequence ions in the range $6 \leqslant Z \leqslant 29$ by means of a distorted-wave Born exchange approximation method including a relativistic correction. The total cross sections include the contributions from direct ionization and excitation autoionization. For excitation autoionization the branching ratio and the configuration interaction are considered. A package of computer codes has been developed and used to calculate these cross sections. Systematic study of the dependence of the cross sections on impact energies and nuclear charges is carried out. The results of the calculations are fitted by empirical formulas to meet the requirements of applications. The fitted values are in good agreement with the calculated results.

0092-640X/96 $18.00

CONTENTS

1. INTRODUCTION

The electron–ion collision is one of the fundamental processes in atomic physics. In astrophysics, plasmas, and x-ray laser studies, large amounts of atomic data are required. Electron impact ionization cross sections are important data in modeling the structure and dynamics of high-temperature plasmas occurring both naturally in space and artificially in fusion devices.[1] In recent years, the study of soft x-ray lasers has made rapid progress.[2,3] The electron impact ionization cross sections for highly charged Li-like ions are very important atomic parameters for the above studies. In many situations, where it is necessary to obtain the data quickly and accurately, a suitable empirical formula for the ionization cross sections becomes very useful.

In this paper, we use a distorted-wave Born exchange (DWBE) approximation method to calculate a series of electron impact ionization cross sections for Li-like ions. This method had been applied successfully in an earlier work[4] to obtain the ionization cross sections for H-like and He-like isoelectronic sequences. The variations of the cross sections with impact energies and nuclear charges are systematically studied, and then empirical formulas are derived to fit the calculated results.

2. OUTLINE OF THE DWBE APPROXIMATION

Our DWBE approximation, described in more detail in our previous works,[5] is a development of the Coulomb–Born (CB) approximation with the following four improvements: (1) we take into account the distortion of the Coulomb potential due to the bound electrons distribution; (2) we include the exchange effect between the two free electrons in the final state; (3) we include the exchange effect between the free electron and bound electrons; and (4) we use a relativistic correction in determining the target electron wave func-

tions.[6] In the outline of the calculation below, atomic units are used.

The total ionization cross section $Q_t(E_i)$ is given by

$$Q_t(E_i) = Q_o(E_i) + Q_i(E_i) + Q_{ea}(E_i), \tag{1}$$

where $Q_o(E_i)$ and $Q_i(E_i)$ are, respectively, the outer-shell and inner-shell direct ionization cross sections from the $1s^2 2s\,^2S_{1/2}$ ground state, and $Q_{ea}(E_i)$ is the excitation autoionization cross section. The latter can be expressed as

$$Q_{ea}(E_i) = \sum_j Q_e^j(E_i) B_j^a, \tag{2}$$

where Q_e^j is the excitation cross section of inner-shell electrons to the autoionizing level j and B_j^a is the branching ratio for autoionization from the level j, written as

$$B_j^a = \frac{\Sigma_m A_a(j \to m)}{\Sigma_m A_a(j \to m) + \Sigma_k A_r(j \to k)}, \tag{3}$$

in which $A_a(j \to m)$ is the autoionization rate to channel m and $A_r(j \to k)$ is radiative transition rate to the bound level k.

2.1. Direct Ionization Cross Section

In the DWBE approximation, the direct ionization cross section (in units of πa_0^2 with a_0 being the Bohr radius) can be written as[5]

$$Q(E_i) = \int_0^{E/2} \sigma(E_e, E_i) dE_e, \tag{4}$$

where E_i and E_e are the incident and ejected electron energies, respectively. E is the sum of the ejected and scattered electron energies in the final state. $\sigma(E_e, E_i)$ is the differential cross section as function of energy. By using a partial wave expansion, the scattering amplitude can be divided into an angular factor and a Slater integral. To do this, we write

$$\sigma(E_e, E_i) = \frac{16}{\pi E_i} \sum_{l_i l_e l_f L} I_{l_i l_e l_f L}(E_e, E_i), \tag{5}$$

where l_i, l_e, and l_f are the angular momenta of incident, ejected, and scattered electrons, respectively, and L is the total angular momentum of the whole system, and

$$I_{l_i l_e l_f L}(E_e, E_i) = |f|^2 + |g|^2 - \alpha |f|\ |g|; \tag{6}$$

f and g are direct and exchange partial wave scattering amplitudes, respectively. Here, we use the maximum interference approximation ($\alpha = 1$)[7] to treat the interaction between the direct and exchange terms, which are written as

$$f = \sum_\lambda f_\lambda(l_b l_i l_e l_f L)\left(P_b P_i \left|\frac{1}{r_{12}}\right| P_e P_f\right)_\lambda \tag{7}$$

$$g = \sum_\lambda f_\lambda(l_b l_i l_f l_e L)\left(P_b P_i \left|\frac{1}{r_{12}}\right| P_f P_e\right)_\lambda, \tag{8}$$

where f_λ is an angular factor in which l_b is the angular momentum of the bound electron, and $(P_b P_i|1/r_{12}|P_e P_f)_\lambda$ is the Slater integral in which P_b, P_i, P_e, and P_f are the radial wave functions of bound, incident, ejected and scattered electrons, respectively. P_b is obtained from the atomic structure program of Cowan[6] in an HFR (Hartree–Fock approximation with relativistic correction) model. The calculations of P_i, P_e, and P_f are included in our own program. The effective integration method has been given in our previous work.[8] The total error introduced by the numerical calculation is estimated at less than 0.5%.

2.2. Excitation Autoionization Cross Section

From Eq. (2) we can see that, in order to get the autoionization cross section, we have to calculate the inner-shell excitation cross section $Q_e^j(E_i)$ to the excited level j, and the autoionization branching ratio B_j^a of the level j. In this paper, the inner-shell excitation cross sections are calculated by using our own program, and the branching ratios are obtained from Cowan's program.[6] In our calculation, the effect of configuration interaction (CI) on the autoionization cross section is also considered.

In the *LS* coupling scheme, the inner-shell excitation cross section for the transition from i to f, that is $Q_e^j(E_i)$ in Eq. (2), can be written as[9,10]

$$Q_e(i \to f) = \frac{2\pi a_0^2}{g_i E_i(\mathrm{Ry})} \sum_J (2J+1) \times \sum_{ll'jj'} |R(\alpha_i L_i S_i J_i l s j J;\ \alpha_f L_f S_f J_f l' s' j' J)|^2, \tag{9}$$

where g_i is the statistical weight of the initial state, E_i (Ry) is the incident energy in rydberg, and J is the total angular momentum of the system. l, l', s, s', j, and j' are, respectively, the orbital, spin and total angular momenta of the incident (unprime) and scattered (prime) electron. L_i, S_i, and J_i are the orbital, spin and total angular momenta of the target ion; α_i represents the other quantum numbers of the target ion. L_f, S_f, J_f, and α_f are the corresponding quantum numbers of the residual ion. The reactance matrix R has a direct and an exchange part:

$$\mathbf{R} = \mathbf{R}^d - \mathbf{R}^e. \tag{10}$$

The exchange scattering matrix element $\mathbf{R}^e$ represents the exchange effect between the scattered electron and the electron in the excited state.

When CI is considered, the new eigenvectors corre-

sponding to the energy level J can be represented by the combination of the eigenvectors in the LS coupling scheme

$$\Phi_J = \sum_{\alpha LS} c(\alpha LS, J)\phi_{\alpha LS}, \tag{11}$$

where $c(\alpha LS, J)$ is the configuration mixing coefficient. Then the excitation cross section should be

$$Q_e(i \to f) = \frac{2\pi a_0^2}{g_i E_i(\mathrm{Ry})} \sum_J (2J + 1) \times \sum_{ll'jj'} \Big| \sum_{\alpha_i L_i S_i \alpha_f L_f S_f} c(i)c(f)R(\alpha_i L_i S_i J_i l s j J;\ \alpha_f L_f S_f J_f l' s' j' J) \Big|^2, \tag{12}$$

where $c(i)$ is the abbreviation for $c(\alpha_i L_i S_i, J_i)$.

3. CALCULATED DIRECT IONIZATION CROSS SECTIONS

3.1. Scaled Cross Sections

In our calculations, we choose ten Li-like ions: C^{3+}, O^{5+}, F^{6+}, Mg^{9+}, Al^{10+}, Si^{11+}, Cl^{14+}, V^{20+}, Fe^{23+} and Cu^{26+}. For the incident electron, we define the reduced incident energy as

$$u = E_i/I, \tag{13}$$

where E_i is the incident energy and I represents the outer-shell ionization potential I_o when calculating Q_o or the inner-shell ionization potential I_i when calculating Q_i for each ion. The values of I_o and I_i, obtained by Cowan's program,[6] are listed in Table I. The energy range in our calculation is from $u = 1.01$ to $u = 15.0$ as required for practical applications. The calculated direct ionization cross sections for the above ions are given in Table II. The choice of 26 incident energy points in the tabulation is to satisfy the requirements for linear interpolation. It should be noted that the scaled cross sections uI^2Q are also given in the tables; the unit of scaled cross sections is $\mathrm{Ry}^2\pi a_0^2$ (Ry is the rydberg energy, a_0 is the Bohr radius). Figures 1 and 2 show, respectively, the dependence of $uI_o^2Q_o$ and $uI_i^2Q_i$ on $1/(Z - 2)$ for Li-like ions. From Figs. 1 and 2, we can see two features: (1) uI^2Q varies only slightly and rather linearly with $1/(Z - 2)$ for an isoelectronic sequence of ions. Hence it is simple to fit the dependence of the scaled cross sections on Z and reasonable to extrapolate the fitting curve to larger Z values. (2) uI^2Q increases monotonically with u and changes more slowly at large u. Thus, fitting to u is relatively easy and appropriate extrapolation to larger u can also be justified.

3.2. Empirical Formula and Fit Parameters for Individual Ions

There are several methods to fit the variation of the cross sections with incident energy for a fixed ion. As discussed in Ref. 4, the best overall fit is given by the following formula by Younger:[11]

$$uI^2Q = A\left(1 - \frac{1}{u}\right) + B\left(1 - \frac{1}{u}\right)^2 + C \ln u + D\,\frac{\ln u}{u}; \tag{14}$$

here A, B, C, and D are four adjustable parameters. The tendencies of the formula at the two limits are

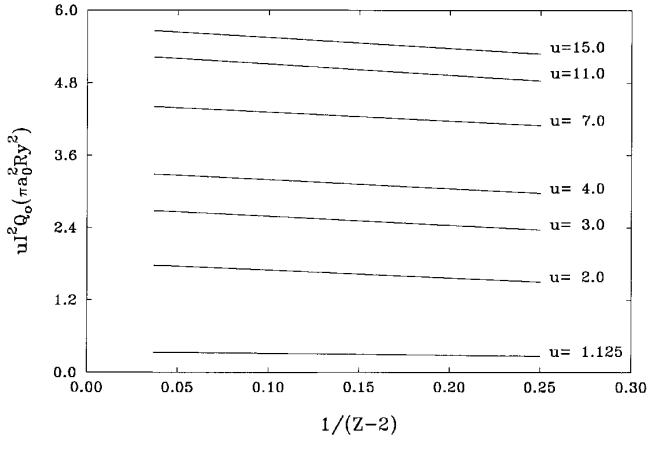

Figure 1. Dependence of the scaled outer-shell direct ionization cross section $uI_o^2Q_o$ on $1/(Z - 2)$.

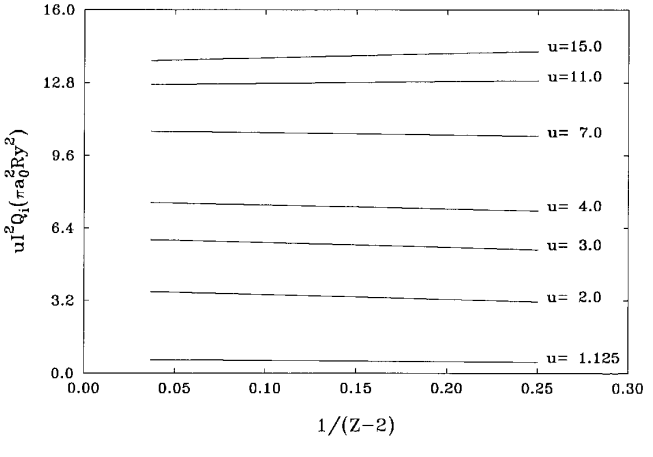

Figure 2. Dependence of the scaled inner-shell direct ionization cross section $uI_i^2Q_i$ on $1/(Z - 2)$.

$$u \to 1 \quad Q \to 0 \tag{15}$$

$$u \to \infty \quad Q \propto \frac{\ln u}{u}\,. \tag{16}$$

Equation (16) has the same form as the well-known Bethe formula.[12]

We use an ''optimal calculation method''[13] to determine the values of the parameters. As we noted in Ref. 4, Younger's formula gives a smaller average deviation than the formulas of Lotz[14] and Sampson.[15] The average deviation F (in percent) is defined as

$$F(\%) = \sqrt{\frac{1}{N}\sum_{i=1}^{N}\left(\frac{Q_{fit}(u) - Q_{cal}(u)}{Q_{cal}(u)}\right)^2} \times 100, \tag{17}$$

where Q_{cal} and Q_{fit} are calculated and fitted values, respectively, and N is the number of calculated points used in making the fit. The fitting parameters and average deviations are given in Table III for outer-shell ionization and in Table IV for inner-shell ionization.

3.3. Fit Parameters for the Isoelectronic Sequence

Because the variation of uI^2Q with $1/(Z-2)$ for Li-like ions is nearly a straight line, we can fit the scaled cross sections to the form

$$uI^2Q = a(u) + b(u)/(Z-2), \tag{18}$$

where a and b are two parameters which depend on the scaled incident energy u only. A formula like Eq. (14) can in turn be used to fit the variation of a and b with u, so that

$$a(u) = A_1\left(1 - \frac{1}{u}\right) + B_1\left(1 - \frac{1}{u}\right)^2 + C_1 \ln u + D_1 \frac{\ln u}{u} \tag{19}$$

$$b(u) = A_2\left(1 - \frac{1}{u}\right) + B_2\left(1 - \frac{1}{u}\right)^2 + C_2 \ln u + D_2 \frac{\ln u}{u}\,, \tag{20}$$

where A_1, B_1, C_1, D_1, A_2, B_2, C_2, and D_2 are adjustable parameters. These fit parameters are given in Table V. One can use these fit parameters, the ionization potentials in Table I, and Eq. (18) to obtain quickly the direct ionization cross section of the other Li-like ions with $Z < 40$ which have not been tabulated. For still higher Z ions, the extrapolation is inappropriate because of the larger relativistic effects.

As a test, we compared the cross sections for electron impact ionization of all 10 Li-like ions obtained from the formulas (18) using the fit parameters in Table V with the calculated values in Table II. We found that the deviations between the fitting results and DWBE calculations are smaller than 1% in most cases and between 1% and 2% for the remaining ones.

4. CALCULATED EXCITATION AUTOIONIZATION CROSS SECTIONS

4.1. Excitation Autoionization Cross Sections with Branching Ratio

In the calculation of excitation autoionization cross sections for Li-like ions, only excitations from the $1s^22s$ ground state to the excited states arising from $1s2s^2$, $1s2s2p$, and $1s2s3p$ are considered. The contributions from other transitions are neglected. Among the above three excitations, the second one makes the largest contribution to the autoionization cross section.

Based on Eq. (12), we calculated the excitation cross sections of inner-shell electrons taking configuration interaction into consideration for the excited state. For the $1s2s^2$ configuration, only the interaction with the configuration $1s2p^2$ was taken into account. For the $1s2s2p$ configuration, we considered the interaction with the configurations $1s2s3p$, $1s2p3s$, and $1s2p3d$. For the $1s2s3p$ configuration, we considered the interaction with the configurations $1s2p3s$ and $1s2p3d$. The branching ratios are also calculated under the same scheme of interacting configurations. It should be pointed out that the excitations via configuration interaction from the ground state to the $1s2p^2$, $1s2p3s$, and $1s2p3d$ states are estimated to be below 5% and are neglected in our calculation.

The configuration $1s2s^2$ has only one level, but the configuration $1s2snp$ has seven levels. Hence there are 15 inner-shell excitation cross section curves for each ion, one for excitation to the $1s2s^2$, seven to the $1s2s2p$, and seven to the $1s2s3p$ levels. In this paper, the autoionization cross section data are treated in three groups according to the configuration to which they belong. Here, we use $Q_e(2s)$, $Q_e(2p)$ and $Q_e(3p)$ to represent the sum of the excitation cross sections to the $1s2s^2$, $1s2s2p$, and $1s2s3p$ configurations, respectively. The excitation autoionization cross sections $Q_{ea}(2s)$, $Q_{ea}(2p)$, and $Q_{ea}(3p)$ are obtained from Eq. (2). As an illustration, we show in Table A the computation of $Q_e(2p)$ and $Q_{ea}(2p)$ for the ion Al^{10+}. Here, the first three rows give the state labels, excitation energies (I_{ex}), and autoionization branching ratios (BR) of the seven states of the $1s2s2p$ configuration. Below each state are listed the excitation cross sections corresponding to incident electron energies E_i. The sum of these cross sections is the excitation cross section for the entire $1s2s2p$ configuration listed under $Q_e(2p)$. By

TABLE A
Excitation Autoionization Cross Sections (in cm^2) for the $1s2s2p$ Configuration of Al^{10+}

State	$(^3S)^2P_{1/2}$	$(^1S)^2P_{1/2}$	$(^3S)^2P_{1/2}$	$(^3S)^4P_{3/2}$	$(^1S)^2P_{3/2}$	$(^3S)^2P_{3/2}$	$(^3S)^4P_{5/2}$		
I_{ex}	1562.7	1579.3	1587.5	1563.1	1579.7	1587.7	1563.6		
BR	0.3118	0.2637	0.9577	0.3192	0.1686	0.9739	0.000		
E_i								Q_e (2p)	Q_{ea} (2p)
1570	7.578E−22	0.0	0.0	1.517E−21	0.0	0.0	2.275E−21	4.550E−21	7.205E−22
1600	7.294E−22	1.797E−21	8.752E−22	1.460E−21	3.699E−21	1.644E−21	2.187E−21	1.239E−20	4.230E−21
2000	4.066E−22	2.123E−21	6.452E−22	8.145E−22	4.418E−21	1.117E−21	1.219E−21	1.074E−20	3.398E−21
4000	5.808E−23	2.401E−21	3.838E−22	1.178E−22	5.039E−21	5.289E−22	1.728E−22	8.701E−21	2.421E−21
6000	1.749E−23	2.181E−21	3.185E−22	3.649E−23	4.579E−21	4.162E−22	5.110E−23	7.600E−21	2.075E−21

combining the individual state excitation cross sections with the branching ratios, the excitation ionization cross sections $Q_{ea}(2p)$ for the entire $1s2s2p$ configuration are obtained. The same method is used to obtain $Q_e(2s)$, $Q_e(3p)$, $Q_{ea}(2s)$, and $Q_{ea}(3p)$. In Table VI, the calculated results for the 10 Li-like ions are given. The total excitation cross sections Q_e and the total autoionization cross section Q_{ea} are the sum of the contributions from these three configurations. The incident energy ranges up to 15 times the outer-shell ionization potential. The distribution of the energy points is chosen to satisfy the requirements of linear interpolation.

4.2. Empirical Formula and Fit Parameters for the Autoionization Cross Sections

We fit the scaled autoionization cross section Z^4Q_{ea} by using the empirical formula

$$Z^4Q_{ea}(u) = A(Z)\left(1 - \frac{1}{u^{40}}\right)\left[\frac{1}{u^{1/3}} + \frac{B(Z)}{u^{4/3}}\right], \quad (21)$$

where A and B are two adjustable parameters which depend on Z, and u is the reduced incident energy given by

$$u = E_i/I_{ex}(2s), \quad (22)$$

where $I_{ex}(2s)$ is the energy of the $1s^22s \rightarrow 1s2s^2$ transition obtained by Cowan's program[6] (see Table VII for the values of $I_{ex}(2s)$).

In Eq. (21), the first factor $A(Z)$ determines the average height of the autoionization cross section curve, the second factor $(1 - 1/u^{40})$ describes the rapid rise of the autoionization cross section curve near threshold, and the third factor $[1/u^{1/3} + B(Z)/u^{4/3}]$ accounts for the decrease of the autoionization cross section past the maximum. The rapidity with which the autoionization cross section decreases varies with the atomic number Z. This is mainly caused by the variation of the branching ratio for autoionization. The parameters A and B are functions of Z, their fitting values are listed in Table VIII. It can also be seen that the variation of A and B with Z is smooth, so it would be reasonable to make interpolations and some modest extrapolation to obtain the autoionization cross sections of ions with $Z < 40$ which have not been tabulated. As an example of a fit, the scaled autoionization cross section of Al^{10+} as a function of u is given in Fig. 3. In the figure, the solid curve is the calculated value and the dashed curve is the fitted one. We can see that the fitting is quite successful. The results of our calculation indicate that the fitting is better when the Z is higher. Except for the near-threshold points, the deviation between the fitted result and the calculated result is less than 5% for $Z > 10$. For $Z < 10$, the deviation can be up to 10%, but compared with the total ionization cross section, this deviation can still be neglected.

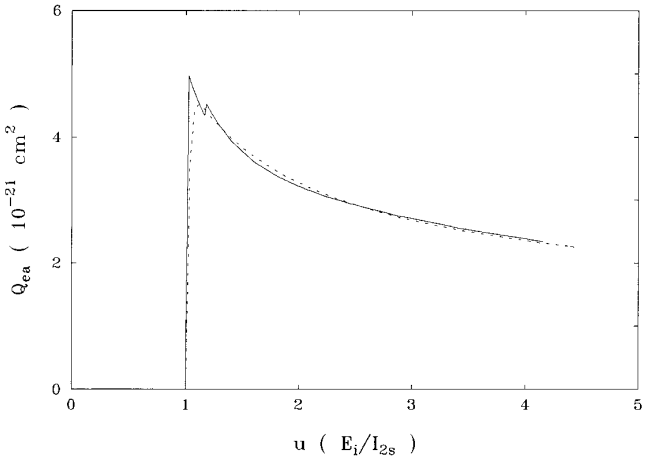

Figure 3. Excitation autoionization cross section for Al^{10+}. The solid curve represents calculated values and the dashed curve represents the fitted values.

5. COMPARISON WITH OTHER WORKS

For low Z Li-like ions, there are some absolute cross section measurements by Crandall et al.[16] for B^{2+}, C^{3+}, N^{4+}, and O^{5+}; Rinn et al.[17] for O^{5+}; Defrance et al.[18] for N^{4+}, O^{5+}, and Ne^{7+}; and Hofmann et al.[19] for B^{2+}, C^{3+}, N^{4+}, O^{5+}, and F^{6+}. The first three experiments agree well with each other. The results of the last experiment are slightly higher than the others, compared with the available data of Crandall and Rinn, the difference is 10% for B^{2+}, and rises up to 25% for the O^{5+} ion.[19] Like other existing nonrelativistic theoretical calculations,[7,20,21] our calculations also agree well with the first three experiments. Compared to Hofmann's experimental data,[19] our direct ionization cross sections are about 20% higher for C^{3+}, and 25%–30% lower for O^{5+} and F^{6+}. As indicated by Reed,[22] for direct ionization cross sections, their calculations with relativistic distorted-wave approximation were 20–25% smaller than Hofmann's data. In Fig. 4, we show the comparison of our results for the total ionization cross section of O^{5+} ions with some available experimental data[16–18] and two other calculations.[20,21] One of the calculations is the Coulomb–Born exchange approximation of Jakubowicz and Moores,[20] and the other is the scaled Coulomb–Born approximation of Sampson and Golden.[21] Both of these calculations include the contribution from excitation autoionization. From the figure, it can be seen that the present calculation shows good agreement with the experiments and the two calculations. We also compared our direct ionization cross sections with Younger's calculations[7] for O^{5+} and Mg^{9+} ions, the difference is within 1.5%.

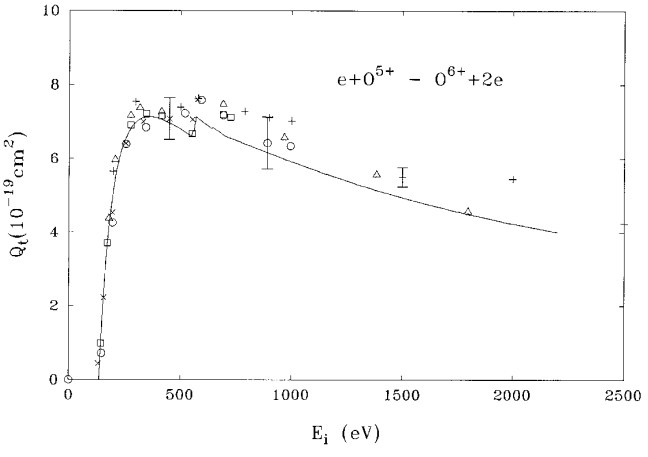

Figure 4. Total ionization cross section (sum of outer shell, excitation autoionization, and inner shell) for O^{5+}. The solid curve represents our results. (○) (Ref. 16), (×) (Ref. 17), and (+) (Ref. 18) are experimental data. (□) (Ref. 20) and (△) (Ref. 21) are other theoretical calculations.

TABLE B
$1s^2s \rightarrow \Sigma_l\ 1s2s2l$ Excitation Autoionization Cross Sections
(in 10^{-19} cm^2) at the Maximum

Ion	Crandall[a]	Rinn[b]	Defrance[c]	Hofmann[d]	Reed[e]	Tayal[f]	Present[g]	Present[h]
C^{3+}	2.3 ± 0.7			2.4 ± 0.2	2.3	2.6	3.0	2.1
N^{4+}	1.6 ± 0.4		1.70 ± 0.46	1.3 ± 0.1	1.4	1.3	1.5	1.1
O^{5+}	0.8 ± 0.3	0.63 ± 0.05	0.62 ± 0.19	0.76 ± 0.08	0.77	0.82	0.93	0.61

[a] From Ref. 16.
[b] The value is estimated from Fig. 2 in Ref. 17.
[c] From Ref. 18.
[d] The values are estimated from Figs. 2, 3, and 4 in Ref. 19.
[e] The values, without radiative decay, are estimated from Figs. 7, 6, and 4 in Ref. 22.
[f] The values, without radiative decay, are estimated from Figs. 2, 3, and 4 in Ref. 23.
[g] Without radiative decay. The value for N^{4+} is from Ref. 24.
[h] With radiative decay.

Table B shows the comparisons of the present $1s^22s \rightarrow \Sigma_l 1s2s2l$ excitation cross sections at the maximum with some measurements and calculations for C^{3+}, N^{4+}, and O^{5+}. The incident electron energies at the maximum are about 305 eV for C^{3+}, 460 eV for N^{4+}, and 570 eV for O^{5+}. The comparisons show that our excitation cross section are in reasonable agreement with the experimental data[16–19] and the recent theoretical calculations.[22,23]

Experimental ionization data for higher Z Li-like ions are very sparse. Recently, K. L. Wong et al.[25] obtained

TABLE C
Electron-Impact Ionization Cross Sections
(in 10^{-21} cm^2) of Lithium-like Ions

Ion	Energy (keV)	Exp[a]	DW1[b]	DW2[c]	Lotz[d]
Ti^{19+}	3.33	6.91 ± 0.65	7.19	7.81	8.04
V^{20+}	3.64	5.58 ± 0.58	5.94	6.40	6.62
Cr^{21+}	3.97	4.81 ± 0.40	4.94	5.35	5.50
Mn^{22+}	4.31	3.99 ± 0.28	4.14	4.44	4.61
Fe^{23+}	4.66	3.72 ± 0.28	3.50	3.80	3.89

[a] Experimental values from Ref. 25.
[b] Present calculated values.
[c] Values from Ref. 25 calculated using the distorted-wave code of Zhang and Sampson.[26]
[d] Values from Ref. 25 calculated using the semiempirical Lotz formula.[14]

the outer-shell electron ionization cross sections at approximately 2.3 times threshold for Ti^{19+}, V^{20+}, Cr^{21+}, Mn^{22+}, and Fe^{23+} ions, by using the electron-beam ion-trap (EBIT) method. The comparison of our calculated results and the measured EBIT data is listed in Table C. This comparison also shows good agreement between our calculation and experiment. The values calculated[25] using the relativistic distorted-wave code of Zhang and Sampson[26] and the semiempirical Lotz formula[14] are also listed in the table.

Acknowledgments

This work was supported by the Natural Science Foundation of China, the Fok Ying Tung Education Foundation, and a research grant from the Chinese Research Association for Atomic and Molecular Data.

References

1. See references in *Electron Impact Ionization,* edited by T. D. Mark and G. H. Dunn (Springer-Verlag, Berlin, 1986)
2. D. L. Matthews et al., Phys. Rev. Lett. **54,** 110 (1985)
3. Zhi-Zhan Xu et al., Appl. Phys. B **50,** 147 (1990)
4. D. Fang et al., ATOMIC DATA AND NUCLEAR DATA TABLES **61,** 91 (1995)
5. D. Fang, W. Hu, J. Tang, Y. Wang, and F. Yang, Phys. Rev. A **47,** 1861 (1993); W. Hu, D. F. Fang, Y. S. Wang, and F. J. Yang, Phys. Rev. A **49,** 989 (1994)
6. R. D. Cowan, *The Theory of Atomic Structure and Spectra* (Univ. of California Press, Berkeley, 1981)
7. S. M. Younger, Phys. Rev. A **22,** 111 (1980); B. C. Griffin, M. S. Pindzola, and C. Bottcher, Phys. Rev. A **36,** 3642 (1987)
8. D. Fang and Y. Wang, J. Phys. B **24,** 1749 (1991)
9. D. H. Sampson, Phys. Rev. A **34,** 986 (1986)
10. Hu Wei et al., Acta Physica Sinica, to be published
11. S. M. Younger, Phys. Rev. A **24,** 1272, 1278 (1981)
12. Yong-Ki Kim, in *Physics of Ion–Ion and Electron–Ion Collisions,* edited by F. Brouillard and J. W. McGowan (Plenum Press, New York, 1983), p. 101
13. Xi Shaolin, *The Optimal Calculation Method* (Shanghai Science and Technology Publishing House, Shanghai, 1980), p. 63
14. W. Lotz, Z. Phys. **216,** 241 (1968)
15. L. B. Golden and D. H. Sampson, J. Phys. B **13,** 2645 (1980)
16. D. H. Crandall et al., Phys. Rev. A **34,** 1757 (1986)
17. K. Rinn et al., Phys. Rev. A **36,** 595 (1987)
18. P. Defrance et al., J. Phys. B **23,** 2333 (1990)
19. G. Hofmann et al., Z. Phys. D **16,** 113 (1990)
20. H. Jakubowicz and D. L. Moores, J. Phys. B **14,** 3733 (1981)
21. D. H. Sampson and L. B. Golden, J. Phys. B **12,** L785 (1979)
22. K. J. Reed and M. H. Chen, Phys. Rev. A **45,** 4519 (1992)
23. S. S. Tayal and R. J. W. Henry, Phys. Rev. A **44,** 2955 (1991)
24. Hu Wei, et al., Acta Physica Sinica **42,** 1416 (1993)
25. K. L. Wong, et al., Phys. Rev. A **48,** 2850 (1993)
26. H. L. Zhang and D. H. Sampson, Phys. Rev. A **42,** 5378 (1990)

EXPLANATION OF TABLES

TABLE I. Ionization Potentials of Li-like Ions

Z Nuclear charge number
I_o Outer-shell ($2s$) ionization potential in Ry (1 Ry = 13.60 eV)
I_i Inner-shell ($1s$) ionization potential in Ry

TABLE II. Direct Ionization Cross Sections for Li-like Ions

Z Nuclear charge number
u Reduced incident energy $u = E_i/I$ (Eq. (13)), where $I = I_o$ ($I = I_i$) for outer- (inner-) shell ionization
$uI_o^2Q_o$ Outer-shell scaled ionization cross section in πa_0^2 Ry^2 ($a_0 = 0.5292 \times 10^{-8}$ cm)
$uI_i^2Q_i$ Inner-shell scaled ionization cross section in πa_0^2 Ry^2
Q_o Outer-shell ionization cross section in cm^2
Q_i Inner-shell ionization cross section in cm^2

TABLE III. Fit Parameters of Outer-Shell Ionization for Individual Ions

See Eq. (14). F(%) is defined in Eq. (17)

TABLE IV. Fit Parameters of Inner-Shell Ionization for Individual Ions

See Eq. (14). F(%) is defined in Eq. (17)

TABLE V. Fit Parameters for the Li Isoelectronic Sequence

See Eqs. (18)–(20)

TABLE VI. Excitation Autoionization Cross Sections for Li-like Ions

Z Nuclear charge number
E_i Incident energy in eV
$Q_e(2s)$ Excitation cross section to the $1s2s^2$ configuration in cm^2
$Q_{ea}(2s)$ Excitation autoionization cross section for the $1s2s^2$ configuration in cm^2
$Q_e(2p)$ Excitation cross section to the $1s2s2p$ configuration in cm^2
$Q_{ea}(2p)$ Excitation autoionization cross section for the $1s2s2p$ configuration in cm^2
$Q_e(3p)$ Excitation cross section to the $1s2s3p$ configuration in cm^2
$Q_{ea}(3p)$ Excitation autoionization cross section for the $1s2s3p$ configuration in cm^2
Q_e Total excitation cross section in cm^2
Q_{ea} Total excitation autoionization cross section in cm^2

TABLE VII. Excitation Energies of the $1s2s^2$ State for Li-like Ions

Z Nuclear charge number
$I_{ex}(2s)$ Excitation energy for the transition $1s^22s \rightarrow 1s2s^2$ in eV

TABLE VIII. Fit Parameters of Excitation Autoionization Cross Sections for Individual Ions

See Eq. (21)

TABLE I. Ionization Potentials of Li-like Ions

See page 309 for Explanation of Tables

Z	I_o	I_i	Z	I_o	I_i	Z	I_o	I_i
3	0.4072	4.751	12	27.06	125.2	21	94.78	409.6
4	1.357	10.10	13	32.54	148.6	22	104.9	451.5
5	2.812	17.45	14	38.53	174.1	23	115.5	495.5
6	4.770	26.81	15	45.03	201.6	24	126.7	541.6
7	7.227	38.17	16	52.03	231.1	25	138.4	589.8
8	10.17	51.54	17	59.55	262.7	26	150.6	640.1
9	13.65	66.92	18	67.59	296.4	27	163.3	692.5
10	17.62	84.31	19	76.13	332.1	28	176.6	747.0
11	22.08	103.7	20	85.20	369.8	29	190.4	803.7

TABLE II. Direct Ionization Cross Sections for Li-like Ions

See page 309 for Explanation of Tables

Z	u	$uI_i^2Q_i$	Q_i	$uI_o^2Q_o$	Q_o	Z	u	$uI_i^2Q_i$	Q_i	$uI_o^2Q_o$	Q_o
6	1.010	0.0412	4.993E-21	0.0278	1.064E-19	9	1.010	0.0452	8.792E-22	0.0325	1.519E-20
	1.125	0.4863	5.291E-20	0.2703	9.291E-19		1.125	0.5352	9.346E-21	0.2997	1.258E-19
	1.250	0.9270	9.077E-20	0.5030	1.556E-18		1.250	1.016	1.597E-20	0.5570	2.104E-19
	1.500	1.733	1.414E-19	0.8954	2.308E-18		1.500	1.883	2.466E-20	0.9836	3.096E-19
	1.750	2.472	1.729E-19	1.225	2.707E-18		1.750	2.655	2.981E-20	1.331	3.591E-19
	2.000	3.166	1.938E-19	1.509	2.918E-18		2.000	3.362	3.303E-20	1.632	3.853E-19
	2.250	3.811	2.073E-19	1.759	3.023E-18		2.250	4.018	3.508E-20	1.897	3.981E-19
	2.500	4.401	2.155E-19	1.991	3.080E-18		2.500	4.618	3.629E-20	2.128	4.019E-19
	2.750	4.939	2.198E-19	2.197	3.089E-18		2.750	5.168	3.692E-20	2.335	4.009E-19
	3.000	5.456	2.226E-19	2.382	3.070E-18		3.000	5.662	3.708E-20	2.490	3.919E-19
	3.250	5.931	2.234E-19	2.549	3.033E-18		3.250	6.115	3.697E-20	2.686	3.903E-19
	3.500	6.375	2.230E-19	2.704	2.987E-18		3.500	6.547	3.675E-20	2.846	3.840E-19
	3.750	6.788	2.216E-19	2.846	2.935E-18		3.750	6.950	3.641E-20	2.992	3.768E-19
	4.000	7.173	2.195E-19	2.980	2.881E-18		4.000	7.330	3.600E-20	3.128	3.693E-19
	4.500	7.870	2.141E-19	3.219	2.766E-18		4.500	8.024	3.503E-20	3.373	3.539E-19
	5.000	8.480	2.076E-19	3.433	2.655E-18		5.000	8.647	3.398E-20	3.592	3.392E-19
	6.000	9.522	1.943E-19	3.801	2.450E-18		6.000	9.727	3.185E-20	3.952	3.110E-19
	7.000	10.42	1.822E-19	4.104	2.267E-18		7.000	10.59	2.972E-20	4.246	2.864E-19
	8.000	11.21	1.715E-19	4.354	2.105E-18		8.000	11.28	2.770E-20	4.444	2.623E-19
	9.000	11.86	1.613E-19	4.564	1.961E-18		9.000	11.86	2.589E-20	4.644	2.437E-19
	10.00	12.41	1.519E-19	4.740	1.833E-18		10.00	12.35	2.426E-20	4.807	2.270E-19
	11.00	12.89	1.434E-19	4.889	1.719E-18		11.00	12.77	2.281E-20	5.001	2.147E-19
	12.00	13.29	1.356E-19	5.020	1.618E-18		12.00	13.12	2.148E-20	5.143	2.024E-19
	13.00	13.66	1.286E-19	5.149	1.532E-18		13.00	13.40	2.025E-20	5.260	1.911E-19
	14.00	13.96	1.221E-19	5.236	1.446E-18		14.00	13.68	1.920E-20	5.332	1.798E-19
	15.00	14.22	1.160E-19	5.318	1.371E-18		15.00	13.91	1.822E-20	5.448	1.715E-19
8	1.010	0.0441	1.446E-21	0.0317	2.659E-20	12	1.010	0.0474	2.634E-22	0.0338	4.021E-21
	1.125	0.5232	1.540E-20	0.2923	2.201E-19		1.125	0.5585	2.786E-21	0.3139	3.353E-20
	1.250	0.9953	2.637E-20	0.5445	3.691E-19		1.250	1.061	4.764E-21	0.5833	5.607E-20
	1.500	1.846	4.076E-20	0.9587	5.415E-19		1.500	1.950	7.297E-21	1.026	8.218E-20
	1.750	2.610	4.940E-20	1.305	6.318E-19		1.750	2.743	8.798E-21	1.383	9.496E-20
	2.000	3.305	5.473E-20	1.602	6.787E-19		2.000	3.451	9.685E-21	1.689	1.015E-19
	2.250	3.948	5.812E-20	1.866	7.027E-19		2.250	4.092	1.021E-20	1.921	1.026E-19
	2.500	4.546	6.023E-20	2.097	7.107E-19		2.500	4.676	1.050E-20	2.191	1.053E-19
	2.750	5.099	6.141E-20	2.303	7.096E-19		2.750	5.220	1.065E-20	2.389	1.044E-19
	3.000	5.612	6.196E-20	2.488	7.027E-19		3.000	5.743	1.074E-20	2.562	1.026E-19
	3.250	6.078	6.194E-20	2.654	6.919E-19		3.250	6.209	1.072E-20	2.727	1.008E-19
	3.500	6.510	6.160E-20	2.810	6.803E-19		3.500	6.635	1.064E-20	2.883	9.897E-20
	3.750	6.913	6.106E-20	2.957	6.681E-19		3.750	7.029	1.052E-20	3.027	9.699E-20
	4.000	7.291	6.037E-20	3.091	6.548E-19		4.000	7.401	1.039E-20	3.161	9.495E-20
	4.500	7.980	5.873E-20	3.338	6.285E-19		4.500	8.071	1.007E-20	3.441	9.188E-20
	5.000	8.602	5.698E-20	3.553	6.021E-19		5.000	8.675	9.738E-21	3.656	8.786E-20
	6.000	9.686	5.347E-20	3.922	5.539E-19		6.000	9.730	9.102E-21	3.992	7.994E-20
	7.000	10.57	5.001E-20	4.220	5.108E-19		7.000	10.59	8.491E-21	4.297	7.376E-20
	8.000	11.31	4.682E-20	4.447	4.710E-19		8.000	11.32	7.942E-21	4.537	6.814E-20
	9.000	11.90	4.379E-20	4.621	4.350E-19		9.000	11.91	7.428E-21	4.720	6.301E-20
	10.00	12.41	4.110E-20	4.788	4.057E-19		10.00	12.41	6.966E-21	4.913	5.903E-20
	11.00	12.83	3.863E-20	4.956	3.818E-19		11.00	12.82	6.541E-21	5.095	5.565E-20
	12.00	13.20	3.643E-20	5.092	3.595E-19		12.00	13.18	6.165E-21	5.230	5.237E-20
	13.00	13.48	3.434E-20	5.200	3.389E-19		13.00	13.47	5.816E-21	5.334	4.930E-20
	14.00	13.75	3.253E-20	5.329	3.225E-19		14.00	13.72	5.501E-21	5.434	4.664E-20
	15.00	13.99	3.089E-20	5.421	3.062E-19		15.00	13.94	5.216E-21	5.521	4.422E-20

TABLE II. Direct Ionization Cross Sections for Li-like Ions

See page 309 for Explanation of Tables

Z	u	$uI_i^2Q_i$	Q_i	$uI_o^2Q_o$	Q_o	Z	u	$uI_i^2Q_i$	Q_i	$uI_o^2Q_o$	Q_o
13	1.010	0.0480	1.894E-22	0.0343	2.822E-21	17	1.010	0.0494	6.240E-23	0.0339	8.327E-22
	1.125	0.5637	1.996E-21	0.3176	2.346E-20		1.125	0.5795	6.572E-22	0.3261	7.192E-21
	1.250	1.071	3.414E-21	0.5883	3.911E-20		1.250	1.097	1.120E-21	0.6022	1.195E-20
	1.500	1.966	5.222E-21	1.036	5.739E-20		1.500	2.012	1.711E-21	1.062	1.757E-20
	1.750	2.762	6.288E-21	1.395	6.624E-20		1.750	2.810	2.049E-21	1.427	2.023E-20
	2.000	3.472	6.917E-21	1.699	7.059E-20		2.000	3.531	2.253E-21	1.735	2.152E-20
	2.250	4.112	7.282E-21	1.930	7.127E-20		2.250	4.191	2.376E-21	2.005	2.211E-20
	2.500	4.697	7.486E-21	2.197	7.302E-20		2.500	4.791	2.445E-21	2.237	2.220E-20
	2.750	5.242	7.595E-21	2.406	7.270E-20		2.750	5.338	2.477E-21	2.444	2.205E-20
	3.000	5.763	7.654E-21	2.598	7.196E-20		3.000	5.823	2.476E-21	2.640	2.183E-20
	3.250	6.228	7.635E-21	2.769	7.079E-20		3.250	6.264	2.459E-21	2.808	2.144E-20
	3.500	6.654	7.575E-21	2.928	6.951E-20		3.500	6.691	2.439E-21	2.964	2.101E-20
	3.750	7.047	7.487E-21	3.074	6.811E-20		3.750	7.090	2.412E-21	3.102	2.052E-20
	4.000	7.414	7.385E-21	3.208	6.664E-20		4.000	7.464	2.381E-21	3.233	2.005E-20
	4.500	8.079	7.153E-21	3.456	6.381E-20		4.500	8.145	2.309E-21	3.481	1.919E-20
	5.000	8.674	6.912E-21	3.656	6.076E-20		5.000	8.751	2.233E-21	3.695	1.833E-20
	6.000	9.721	6.455E-21	4.022	5.570E-20		6.000	9.789	2.082E-21	4.063	1.680E-20
	7.000	10.58	6.022E-21	4.315	5.122E-20		7.000	10.62	1.936E-21	4.355	1.544E-20
	8.000	11.32	5.638E-21	4.553	4.729E-20		8.000	11.26	1.796E-21	4.598	1.426E-20
	9.000	11.92	5.277E-21	4.797	4.429E-20		9.000	11.81	1.674E-21	4.790	1.320E-20
	10.00	12.41	4.945E-21	4.952	4.115E-20		10.00	12.29	1.568E-21	4.994	1.239E-20
	11.00	12.83	4.647E-21	5.111	3.861E-20		11.00	12.68	1.471E-21	5.147	1.161E-20
	12.00	13.19	4.379E-21	5.272	3.650E-20		12.00	13.03	1.385E-21	5.279	1.091E-20
	13.00	13.47	4.128E-21	5.379	3.438E-20		13.00	13.30	1.305E-21	5.389	1.028E-20
	14.00	13.73	3.907E-21	5.481	3.253E-20		14.00	13.56	1.236E-21	5.493	9.734E-21
	15.00	13.94	3.703E-21	5.565	3.083E-20		15.00	13.77	1.171E-21	5.578	9.226E-21
14	1.010	0.0484	1.391E-22	0.0344	2.018E-21	23	1.010	0.0501	1.778E-23	0.0331	2.161E-22
	1.125	0.5687	1.467E-21	0.3201	1.686E-20		1.125	0.5929	1.889E-22	0.3346	1.962E-21
	1.250	1.078	2.503E-21	0.5925	2.809E-20		1.250	1.121	3.214E-22	0.6191	3.266E-21
	1.500	1.982	3.835E-21	1.044	4.125E-20		1.500	2.050	4.897E-22	1.084	4.766E-21
	1.750	2.773	4.599E-21	1.384	4.687E-20		1.750	2.857	5.850E-22	1.429	5.385E-21
	2.000	3.492	5.068E-21	1.710	5.067E-20		2.000	3.583	6.420E-22	1.760	5.804E-21
	2.250	4.151	5.355E-21	1.978	5.210E-20		2.250	4.233	6.742E-22	2.025	5.936E-21
	2.500	4.750	5.515E-21	2.196	5.206E-20		2.500	4.829	6.922E-22	2.250	5.936E-21
	2.750	5.299	5.593E-21	2.408	5.189E-20		2.750	5.370	6.998E-22	2.459	5.897E-21
	3.000	5.786	5.598E-21	2.612	5.160E-20		3.000	5.873	7.015E-22	2.670	5.870E-21
	3.250	6.231	5.565E-21	2.781	5.071E-20		3.250	6.331	6.981E-22	2.840	5.763E-21
	3.500	6.659	5.522E-21	2.940	4.978E-20		3.500	6.752	6.913E-22	2.993	5.640E-21
	3.750	7.057	5.462E-21	3.086	4.877E-20		3.750	7.142	6.825E-22	3.144	5.529E-21
	4.000	7.431	5.392E-21	3.221	4.772E-20		4.000	7.506	6.724E-22	3.281	5.410E-21
	4.500	8.113	5.233E-21	3.454	4.549E-20		4.500	8.172	6.508E-22	3.526	5.168E-21
	5.000	8.725	5.065E-21	3.657	4.335E-20		5.000	8.768	6.284E-22	3.737	4.929E-21
	6.000	9.776	4.729E-21	4.033	3.984E-20		6.000	9.784	5.843E-22	4.079	4.484E-21
	7.000	10.62	4.404E-21	4.330	3.666E-20		7.000	10.60	5.426E-22	4.370	4.117E-21
	8.000	11.27	4.089E-21	4.562	3.380E-20		8.000	11.28	5.053E-22	4.649	3.833E-21
	9.000	11.83	3.815E-21	4.808	3.166E-20		9.000	11.86	4.722E-22	4.873	3.571E-21
	10.00	12.30	3.570E-21	4.991	2.958E-20		10.00	12.36	4.429E-22	5.031	3.318E-21
	11.00	12.70	3.351E-21	5.117	2.757E-20		11.00	12.80	4.170E-22	5.233	3.137E-21
	12.00	13.05	3.157E-21	5.279	2.607E-20		12.00	13.15	3.927E-22	5.377	2.955E-21
	13.00	13.32	2.974E-21	5.379	2.452E-20		13.00	13.45	3.707E-22	5.506	2.793E-21
	14.00	13.58	2.816E-21	5.482	2.321E-20		14.00	13.71	3.509E-22	5.615	2.645E-21
	15.00	13.80	2.670E-21	5.567	2.199E-20		15.00	13.93	3.328E-22	5.705	2.508E-21

TABLE II. Direct Ionization Cross Sections for Li-like Ions

See page 309 for Explanation of Tables

Z	u	$uI_i^2Q_i$	Q_i	$uI_o^2Q_o$	Q_o	Z	u	$uI_i^2Q_i$	Q_i	$uI_o^2Q_o$	Q_o
26	1.010	0.0509	1.082E-23	0.0322	1.237E-22	29	1.010	0.0511	6.891E-24	0.0321	7.713E-23
	1.125	0.5965	1.139E-22	0.3369	1.162E-21		1.125	0.6002	7.267E-23	0.3390	7.313E-22
	1.250	1.128	1.938E-22	0.6239	1.936E-21		1.250	1.133	1.235E-22	0.6268	1.217E-21
	1.500	2.059	2.948E-22	1.091	2.821E-21		1.500	2.070	1.880E-22	1.094	1.770E-21
	1.750	2.869	3.520E-22	1.430	3.170E-21		1.750	2.882	2.243E-22	1.438	1.994E-21
	2.000	3.601	3.866E-22	1.772	3.437E-21		2.000	3.612	2.460E-22	1.782	2.162E-21
	2.250	4.262	4.067E-22	2.029	3.498E-21		2.250	4.274	2.587E-22	2.055	2.217E-21
	2.500	4.859	4.174E-22	2.258	3.504E-21		2.500	4.874	2.656E-22	2.279	2.212E-21
	2.750	5.404	4.220E-22	2.468	3.481E-21		2.750	5.421	2.685E-22	2.489	2.197E-21
	3.000	5.887	4.214E-22	2.680	3.465E-21		3.000	5.903	2.680E-22	2.693	2.179E-21
	3.250	6.326	4.180E-22	2.850	3.402E-21		3.250	6.347	2.660E-22	2.864	2.139E-21
	3.500	6.753	4.143E-22	3.010	3.336E-21		3.500	6.770	2.635E-22	3.020	2.094E-21
	3.750	7.150	4.094E-22	3.153	3.262E-21		3.750	7.166	2.603E-22	3.168	2.050E-21
	4.000	7.522	4.038E-22	3.288	3.189E-21		4.000	7.536	2.566E-22	3.304	2.005E-21
	4.500	8.200	3.913E-22	3.538	3.050E-21		4.500	8.211	2.485E-22	3.559	1.919E-21
	5.000	8.801	3.780E-22	3.741	2.902E-21		5.000	8.815	2.401E-22	3.766	1.828E-21
	6.000	9.832	3.519E-22	4.102	2.652E-21		6.000	9.851	2.236E-22	4.133	1.672E-21
	7.000	10.65	3.267E-22	4.404	2.441E-21		7.000	10.68	2.078E-22	4.435	1.538E-21
	8.000	11.28	3.028E-22	4.674	2.266E-21		8.000	11.33	1.929E-22	4.688	1.422E-21
	9.000	11.83	2.823E-22	4.922	2.121E-21		9.000	11.89	1.799E-22	4.930	1.329E-21
	10.00	12.30	2.641E-22	5.107	1.981E-21		10.00	12.36	1.684E-22	5.112	1.241E-21
	11.00	12.69	2.477E-22	5.266	1.857E-21		11.00	12.76	1.580E-22	5.265	1.162E-21
	12.00	13.04	2.333E-22	5.401	1.746E-21		12.00	13.10	1.487E-22	5.402	1.093E-21
	13.00	13.30	2.197E-22	5.518	1.647E-21		13.00	13.37	1.401E-22	5.510	1.029E-21
	14.00	13.55	2.078E-22	5.619	1.557E-21		14.00	13.62	1.325E-22	5.611	9.727E-22
	15.00	13.77	1.971E-22	5.703	1.475E-21		15.00	13.84	1.257E-22	5.696	9.216E-22

TABLE III. Fit Parameters of Outer-Shell Ionization for Individual Ions

See page 309 for Explanation of Tables

Z	A	B	C	D	F(%)
6	8.142	-3.067	0.5815	-6.346	0.28
8	7.996	-2.849	0.5623	-5.984	0.27
9	8.101	-2.900	0.5539	-6.003	0.44
12	8.204	-3.080	0.6092	-5.999	0.57
13	7.953	-2.955	0.6570	-5.777	0.50
14	8.239	-3.067	0.6121	-5.995	0.40
17	8.211	-2.991	0.5904	-5.886	0.57
23	8.330	-3.245	0.6774	-5.992	0.51
26	8.165	-3.214	0.7286	-5.857	0.44
29	8.098	-3.079	0.6997	-5.760	0.41

TABLE IV. Fit Parameters of Inner-Shell Ionization for Individual Ions

See page 309 for Explanation of Tables

Z	A	B	C	D	F(%)
6	24.29	-10.41	1.719	-21.83	0.25
8	24.10	-9.862	1.515	-21.12	0.53
9	23.73	-9.420	1.431	-20.57	0.55
12	23.67	-9.425	1.438	-20.28	0.51
13	23.72	-9.454	1.431	-20.26	0.49
14	23.32	-8.882	1.295	-19.73	0.53
17	23.29	-8.798	1.256	-19.55	0.51
23	23.47	-9.058	1.322	-19.64	0.50
26	23.27	-8.674	1.203	-19.32	0.50
29	23.43	-8.850	1.242	-19.48	0.50

TABLE V. Fit Parameters for the Li Isoelectronic Sequence

See page 309 for Explanation of Tables

$a(u)$	A_1	B_1	C_1	D_1
Outer-shell	6.522	-2.370	0.9364	-4.356
Inner-shell	25.54	-9.458	0.7530	-20.95
$b(u)$	A_2	B_2	C_2	D_2
Outer-shell	10.46	-4.351	-2.162	-11.18
Inner-shell	-22.92	4.733	6.368	11.21

TABLE VI. Excitation Autoionization Cross Sections for Li-like Ions

See page 309 for Explanation of Tables

Z	Ei	$Q_e(2s)$	$Q_{ea}(2s)$	$Q_e(2p)$	$Q_{ea}(2p)$	$Q_e(3p)$	$Q_{ea}(3p)$	Q_e	Q_{ea}
6	2.920E+02	0.0	0.0	0.0	0.0	0.0	0.0	0.0	0.0
	2.950E+02	1.641E-20	1.640E-20	1.318E-19	5.022E-20	0.0	0.0	1.482E-19	6.663E-20
	3.050E+02	1.588E-20	1.587E-20	2.799E-19	1.962E-19	0.0	0.0	2.958E-19	2.121E-19
	3.200E+02	1.529E-20	1.528E-20	2.657E-19	1.904E-19	0.0	0.0	2.810E-19	2.057E-19
	3.350E+02	1.450E-20	1.449E-20	2.551E-19	1.868E-19	0.0	0.0	2.696E-19	2.013E-19
	3.380E+02	1.449E-20	1.448E-20	2.534E-19	1.863E-19	3.686E-20	1.844E-20	3.048E-19	2.192E-19
	3.450E+02	1.417E-20	1.416E-20	2.490E-19	1.847E-19	4.426E-20	2.203E-20	3.074E-19	2.209E-19
	3.750E+02	1.296E-20	1.295E-20	2.353E-19	1.810E-19	4.035E-20	2.084E-20	2.886E-19	2.148E-19
	4.000E+02	1.220E-20	1.219E-20	2.273E-19	1.794E-19	3.819E-20	2.028E-20	2.777E-19	2.119E-19
	4.500E+02	1.082E-20	1.081E-20	2.165E-19	1.776E-19	3.537E-20	1.966E-20	2.627E-19	2.081E-19
	5.000E+02	9.591E-21	9.586E-21	2.100E-19	1.771E-19	3.373E-20	1.938E-20	2.533E-19	2.061E-19
	5.500E+02	8.654E-21	8.650E-21	2.054E-19	1.766E-19	3.266E-20	1.923E-20	2.467E-19	2.045E-19
	6.000E+02	7.934E-21	7.930E-21	2.014E-19	1.757E-19	3.196E-20	1.916E-20	2.413E-19	2.028E-19
	6.500E+02	7.262E-21	7.258E-21	1.986E-19	1.750E-19	3.134E-20	1.903E-20	2.372E-19	2.013E-19
	7.000E+02	6.664E-21	6.661E-21	1.958E-19	1.739E-19	3.091E-20	1.896E-20	2.334E-19	1.995E-19
	7.500E+02	6.268E-21	6.265E-21	1.925E-19	1.720E-19	3.040E-20	1.878E-20	2.292E-19	1.970E-19
	8.000E+02	5.823E-21	5.820E-21	1.901E-19	1.706E-19	3.002E-20	1.866E-20	2.259E-19	1.951E-19
	8.500E+02	5.411E-21	5.408E-21	1.877E-19	1.691E-19	2.964E-20	1.850E-20	2.228E-19	1.930E-19
	9.000E+02	5.091E-21	5.088E-21	1.846E-19	1.668E-19	2.918E-20	1.827E-20	2.189E-19	1.902E-19
	1.000E+03	4.605E-21	4.603E-21	1.789E-19	1.622E-19	2.840E-20	1.788E-20	2.119E-19	1.847E-19
8	5.500E+02	0.0	0.0	0.0	0.0	0.0	0.0	0.0	0.0
	5.550E+02	5.245E-21	5.237E-21	3.706E-20	1.275E-20	0.0	0.0	4.230E-20	1.799E-20
	5.600E+02	5.203E-21	5.195E-21	3.661E-20	1.260E-20	0.0	0.0	4.181E-20	1.780E-20
	5.700E+02	5.166E-21	5.158E-21	8.800E-20	5.567E-20	0.0	0.0	9.317E-20	6.084E-20
	5.900E+02	5.012E-21	5.004E-21	8.505E-20	5.442E-20	0.0	0.0	9.006E-20	5.943E-20
	6.390E+02	4.587E-21	4.580E-21	7.985E-20	5.228E-20	0.0	0.0	8.444E-20	5.687E-20
	6.450E+02	4.545E-21	4.538E-21	7.936E-20	5.211E-20	1.141E-20	4.538E-21	9.531E-20	6.119E-20
	6.550E+02	4.508E-21	4.501E-21	7.853E-20	5.178E-20	1.413E-20	4.619E-21	9.717E-20	6.091E-20
	7.000E+02	4.196E-21	4.190E-21	7.546E-20	5.065E-20	1.317E-20	4.348E-21	9.283E-20	5.919E-20
	8.000E+02	3.674E-21	3.668E-21	7.092E-20	4.907E-20	1.192E-20	4.007E-21	8.651E-20	5.675E-20
	9.000E+02	3.261E-21	3.256E-21	6.815E-20	4.816E-20	1.122E-20	3.826E-21	8.263E-20	5.525E-20
	1.000E+03	2.930E-21	2.926E-21	6.622E-20	4.749E-20	1.077E-20	3.707E-21	7.992E-20	5.413E-20
	1.150E+03	2.520E-21	2.516E-21	6.419E-20	4.671E-20	1.034E-20	3.592E-21	7.705E-20	5.282E-20
	1.285E+03	2.251E-21	2.248E-21	6.268E-20	4.598E-20	1.004E-20	3.507E-21	7.497E-20	5.174E-20
	1.400E+03	2.053E-21	2.050E-21	6.138E-20	4.525E-20	9.860E-21	3.453E-21	7.329E-20	5.076E-20
	1.500E+03	1.930E-21	1.927E-21	6.024E-20	4.455E-20	9.672E-21	3.394E-21	7.184E-20	4.987E-20
	1.600E+03	1.794E-21	1.791E-21	5.936E-20	4.401E-20	9.524E-21	3.348E-21	7.068E-20	4.915E-20
	1.800E+03	1.581E-21	1.579E-21	5.726E-20	4.261E-20	9.212E-21	3.243E-21	6.805E-20	4.743E-20
	2.000E+03	1.432E-21	1.430E-21	5.528E-20	4.123E-20	8.920E-21	3.146E-21	6.563E-20	4.581E-20
	2.200E+03	1.284E-21	1.282E-21	5.356E-20	4.001E-20	8.642E-21	3.049E-21	6.349E-20	4.434E-20
9	7.140E+02	0.0	0.0	0.0	0.0	0.0	0.0	0.0	0.0
	7.200E+02	3.275E-21	3.267E-21	2.207E-20	6.544E-21	0.0	0.0	2.534E-20	9.819E-21
	7.350E+02	3.229E-21	3.221E-21	5.472E-20	3.054E-20	0.0	0.0	5.795E-20	3.377E-20
	7.750E+02	3.054E-21	3.047E-21	5.202E-20	2.931E-20	0.0	0.0	5.507E-20	3.236E-20
	8.250E+02	2.856E-21	2.849E-21	4.976E-20	2.832E-20	0.0	0.0	5.262E-20	3.118E-20
	8.350E+02	2.834E-21	2.827E-21	4.942E-20	2.819E-20	7.031E-21	2.378E-21	5.928E-20	3.340E-20
	8.450E+02	2.809E-21	2.802E-21	4.903E-20	2.802E-20	8.842E-21	2.400E-21	6.068E-20	3.323E-20
	9.000E+02	2.625E-21	2.619E-21	4.728E-20	2.728E-20	8.266E-21	2.258E-21	5.817E-20	3.216E-20
	1.000E+03	2.370E-21	2.364E-21	4.499E-20	2.632E-20	7.634E-21	2.105E-21	5.499E-20	3.080E-20
	1.100E+03	2.144E-21	2.139E-21	4.346E-20	2.569E-20	7.229E-21	2.008E-21	5.283E-20	2.984E-20
	1.200E+03	1.970E-21	1.965E-21	4.232E-20	2.521E-20	6.950E-21	1.941E-21	5.124E-20	2.912E-20
	1.300E+03	1.821E-21	1.817E-21	4.137E-20	2.480E-20	6.739E-21	1.891E-21	4.993E-20	2.851E-20
	1.400E+03	1.683E-21	1.679E-21	4.072E-20	2.453E-20	6.584E-21	1.852E-21	4.899E-20	2.806E-20
	1.650E+03	1.429E-21	1.426E-21	3.916E-20	2.377E-20	6.297E-21	1.781E-21	4.689E-20	2.698E-20
	1.800E+03	1.298E-21	1.295E-21	3.836E-20	2.335E-20	6.173E-21	1.750E-21	4.583E-20	2.640E-20

TABLE VI. Excitation Autoionization Cross Sections for Li-like Ions

See page 309 for Explanation of Tables

Z	E_i	$Q_e(2s)$	$Q_{ea}(2s)$	$Q_e(2p)$	$Q_{ea}(2p)$	$Q_e(3p)$	$Q_{ea}(3p)$	Q_e	Q_{ea}
9	2.000E+03	1.177E-21	1.174E-21	3.724E-20	2.274E-20	5.994E-21	1.702E-21	4.441E-20	2.562E-20
	2.200E+03	1.056E-21	1.053E-21	3.633E-20	2.223E-20	5.852E-21	1.664E-21	4.324E-20	2.495E-20
	2.400E+03	9.688E-22	9.665E-22	3.524E-20	2.159E-20	5.689E-21	1.618E-21	4.190E-20	2.418E-20
	2.600E+03	8.989E-22	8.967E-22	3.429E-20	2.102E-20	5.545E-21	1.579E-21	4.073E-20	2.350E-20
	2.800E+03	8.289E-22	8.269E-22	3.346E-20	2.053E-20	5.413E-21	1.541E-21	3.970E-20	2.290E-20
12	1.319E+03	0.0	0.0	0.0	0.0	0.0	0.0	0.0	0.0
	1.330E+03	1.033E-21	1.025E-21	6.375E-21	1.203E-21	0.0	0.0	7.408E-21	2.236E-21
	1.345E+03	1.021E-21	1.013E-21	1.712E-20	6.550E-21	0.0	0.0	1.814E-20	7.571E-21
	1.400E+03	9.840E-22	9.767E-22	1.660E-20	6.315E-21	0.0	0.0	1.758E-20	7.299E-21
	1.500E+03	9.237E-22	9.169E-22	1.579E-20	5.909E-21	0.0	0.0	1.671E-20	6.833E-21
	1.535E+03	8.986E-22	8.920E-22	1.559E-20	5.799E-21	0.0	0.0	1.649E-20	6.698E-21
	1.560E+03	8.845E-22	8.780E-22	1.545E-20	5.728E-21	2.770E-21	4.169E-22	1.910E-20	7.029E-21
	1.600E+03	8.673E-22	8.609E-22	1.522E-20	5.609E-21	2.697E-21	4.054E-22	1.878E-20	6.882E-21
	1.800E+03	7.675E-22	7.618E-22	1.440E-20	5.176E-21	2.455E-21	3.698E-22	1.762E-20	6.313E-21
	2.000E+03	6.932E-22	6.881E-22	1.384E-20	4.882E-21	2.306E-21	3.474E-22	1.684E-20	5.923E-21
	2.200E+03	6.331E-22	6.284E-22	1.341E-20	4.663E-21	2.207E-21	3.327E-22	1.625E-20	5.629E-21
	2.500E+03	5.577E-22	5.536E-22	1.294E-20	4.435E-21	2.108E-21	3.180E-22	1.561E-20	5.311E-21
	2.750E+03	5.029E-22	4.992E-22	1.267E-20	4.303E-21	2.047E-21	3.086E-22	1.522E-20	5.114E-21
	3.000E+03	4.650E-22	4.616E-22	1.237E-20	4.174E-21	2.002E-21	3.019E-22	1.484E-20	4.941E-21
	3.300E+03	4.194E-22	4.163E-22	1.210E-20	4.060E-21	1.949E-21	2.939E-22	1.447E-20	4.773E-21
	3.600E+03	3.863E-22	3.834E-22	1.177E-20	3.935E-21	1.905E-21	2.872E-22	1.406E-20	4.608E-21
	4.000E+03	3.474E-22	3.448E-22	1.144E-20	3.808E-21	1.846E-21	2.784E-22	1.363E-20	4.434E-21
	4.500E+03	3.074E-22	3.051E-22	1.097E-20	3.644E-21	1.780E-21	2.682E-22	1.306E-20	4.220E-21
	5.000E+03	2.792E-22	2.771E-22	1.056E-20	3.500E-21	1.715E-21	2.585E-22	1.255E-20	4.038E-21
	5.500E+03	2.513E-22	2.494E-22	1.019E-20	3.373E-21	1.657E-21	2.497E-22	1.210E-20	3.874E-21
13	1.560E+03	0.0	0.0	0.0	0.0	0.0	0.0	0.0	0.0
	1.570E+03	7.445E-22	7.369E-22	4.550E-21	7.205E-22	0.0	0.0	5.294E-21	1.465E-21
	1.600E+03	7.361E-22	7.286E-22	1.239E-20	4.230E-21	0.0	0.0	1.313E-20	4.966E-21
	1.650E+03	7.155E-22	7.082E-22	1.205E-20	4.078E-21	0.0	0.0	1.277E-20	4.794E-21
	1.750E+03	6.747E-22	6.678E-22	1.156E-20	3.827E-21	0.0	0.0	1.223E-20	4.502E-21
	1.820E+03	6.517E-22	6.451E-22	1.129E-20	3.684E-21	0.0	0.0	1.194E-20	4.336E-21
	1.850E+03	6.396E-22	6.331E-22	1.119E-20	3.632E-21	2.022E-21	2.479E-22	1.385E-20	4.520E-21
	1.900E+03	6.269E-22	6.205E-22	1.101E-20	3.543E-21	1.965E-21	2.407E-22	1.360E-20	4.411E-21
	2.000E+03	5.923E-22	5.863E-22	1.074E-20	3.398E-21	1.876E-21	2.301E-22	1.321E-20	4.220E-21
	2.200E+03	5.387E-22	5.332E-22	1.031E-20	3.169E-21	1.755E-21	2.155E-22	1.260E-20	3.923E-21
	2.500E+03	4.764E-22	4.715E-22	9.850E-21	2.931E-21	1.641E-21	2.017E-22	1.197E-20	3.609E-21
	2.800E+03	4.244E-22	4.201E-22	9.545E-21	2.775E-21	1.565E-21	1.926E-22	1.153E-20	3.392E-21
	3.100E+03	3.863E-22	3.824E-22	9.290E-21	2.657E-21	1.513E-21	1.863E-22	1.119E-20	3.230E-21
	3.500E+03	3.422E-22	3.387E-22	8.992E-21	2.533E-21	1.460E-21	1.798E-22	1.079E-20	3.055E-21
	4.000E+03	2.976E-22	2.946E-22	8.701E-21	2.421E-21	1.407E-21	1.733E-22	1.041E-20	2.892E-21
	4.500E+03	2.671E-22	2.644E-22	8.391E-21	2.317E-21	1.359E-21	1.673E-22	1.002E-20	2.751E-21
	5.000E+03	2.380E-22	2.356E-22	8.134E-21	2.234E-21	1.318E-21	1.623E-22	9.690E-21	2.634E-21
	5.500E+03	2.173E-22	2.151E-22	7.844E-21	2.147E-21	1.274E-21	1.569E-22	9.335E-21	2.521E-21
	6.000E+03	2.004E-22	1.984E-22	7.600E-21	2.075E-21	1.236E-21	1.522E-22	9.036E-21	2.428E-21
	6.500E+03	1.836E-22	1.817E-22	7.375E-21	2.010E-21	1.200E-21	1.478E-22	8.759E-21	2.341E-21
14	1.825E+03	0.0	0.0	0.0	0.0	0.0	0.0	0.0	0.0
	1.840E+03	5.529E-22	5.454E-22	3.310E-21	4.395E-22	0.0	0.0	3.863E-21	9.924E-22
	1.860E+03	5.509E-22	5.434E-22	9.194E-21	2.830E-21	0.0	0.0	9.745E-21	3.381E-21
	1.900E+03	5.405E-22	5.331E-22	9.054E-21	2.777E-21	0.0	0.0	9.595E-21	3.318E-21
	2.000E+03	5.136E-22	5.066E-22	8.691E-21	2.604E-21	0.0	0.0	9.205E-21	3.118E-21
	2.130E+03	4.828E-22	4.762E-22	8.369E-21	2.434E-21	0.0	0.0	8.852E-21	2.917E-21
	2.150E+03	4.768E-22	4.703E-22	8.330E-21	2.412E-21	1.494E-21	1.518E-22	1.030E-20	3.041E-21
	2.200E+03	4.677E-22	4.613E-22	8.221E-21	2.358E-21	1.476E-21	1.491E-22	1.016E-20	2.975E-21
	2.500E+03	4.119E-22	4.063E-22	7.747E-21	2.107E-21	1.330E-21	1.347E-22	9.489E-21	2.654E-21

TABLE VI. Excitation Autoionization Cross Sections for Li-like Ions

See page 309 for Explanation of Tables

Z	Ei	Q_e(2s)	Q_{ea}(2s)	Q_e(2p)	Q_{ea}(2p)	Q_e(3p)	Q_{ea}(3p)	Q_e	Q_{ea}
14	2.800E+03	3.683E-22	3.633E-22	7.429E-21	1.942E-21	1.244E-21	1.261E-22	9.041E-21	2.436E-21
	3.200E+03	3.230E-22	3.186E-22	7.133E-21	1.796E-21	1.174E-21	1.191E-22	8.630E-21	2.238E-21
	3.600E+03	2.892E-22	2.853E-22	6.904E-21	1.693E-21	1.127E-21	1.144E-22	8.320E-21	2.097E-21
	4.000E+03	2.591E-22	2.556E-22	6.716E-21	1.618E-21	1.090E-21	1.108E-22	8.065E-21	1.988E-21
	4.400E+03	2.367E-22	2.335E-22	6.558E-21	1.559E-21	1.061E-21	1.078E-22	7.856E-21	1.904E-21
	5.000E+03	2.078E-22	2.050E-22	6.314E-21	1.482E-21	1.025E-21	1.041E-22	7.547E-21	1.794E-21
	5.500E+03	1.902E-22	1.876E-22	6.143E-21	1.431E-21	9.943E-22	1.011E-22	7.327E-21	1.722E-21
	6.000E+03	1.726E-22	1.703E-22	5.970E-21	1.383E-21	9.690E-22	9.848E-23	7.112E-21	1.654E-21
	6.500E+03	1.602E-22	1.580E-22	5.787E-21	1.336E-21	9.409E-22	9.561E-23	6.888E-21	1.592E-21
	7.000E+03	1.494E-22	1.474E-22	5.632E-21	1.296E-21	9.161E-22	9.311E-23	6.697E-21	1.539E-21
	7.800E+03	1.331E-22	1.313E-22	5.401E-21	1.239E-21	8.798E-22	8.940E-23	6.414E-21	1.462E-21
17	2.740E+03	0.0	0.0	0.0	0.0	0.0	0.0	0.0	0.0
	2.750E+03	2.496E-22	2.425E-22	1.464E-21	1.142E-22	0.0	0.0	1.714E-21	3.638E-22
	2.780E+03	2.526E-22	2.455E-22	4.190E-21	1.012E-21	0.0	0.0	4.443E-21	1.265E-21
	2.850E+03	2.465E-22	2.395E-22	4.131E-21	9.924E-22	0.0	0.0	4.377E-21	1.239E-21
	2.950E+03	2.384E-22	2.317E-22	4.022E-21	9.449E-22	0.0	0.0	4.260E-21	1.183E-21
	3.210E+03	2.194E-22	2.132E-22	3.820E-21	8.487E-22	0.0	0.0	4.039E-21	1.068E-21
	3.240E+03	2.173E-22	2.112E-22	3.803E-21	8.398E-22	6.891E-22	4.251E-23	4.709E-21	1.100E-21
	3.300E+03	2.133E-22	2.073E-22	3.765E-21	8.221E-22	6.791E-22	4.185E-23	4.657E-21	1.077E-21
	3.500E+03	2.013E-22	1.956E-22	3.658E-21	7.703E-22	6.431E-22	3.979E-23	4.502E-21	1.011E-21
	4.000E+03	1.774E-22	1.724E-22	3.456E-21	6.760E-22	5.876E-22	3.668E-23	4.221E-21	8.901E-22
	4.500E+03	1.579E-22	1.534E-22	3.323E-21	6.151E-22	5.538E-22	3.478E-23	4.035E-21	8.078E-22
	5.000E+03	1.420E-22	1.380E-22	3.227E-21	5.733E-22	5.304E-22	3.346E-23	3.899E-21	7.488E-22
	5.500E+03	1.299E-22	1.262E-22	3.144E-21	5.417E-22	5.132E-22	3.248E-23	3.787E-21	7.041E-22
	6.500E+03	1.104E-22	1.073E-22	3.004E-21	4.972E-22	4.877E-22	3.098E-23	3.602E-21	6.386E-22
	7.000E+03	1.021E-22	9.921E-23	2.948E-21	4.815E-22	4.766E-22	3.032E-23	3.527E-21	6.139E-22
	8.000E+03	8.996E-23	8.741E-23	2.824E-21	4.527E-22	4.578E-22	2.917E-23	3.372E-21	5.718E-22
	9.000E+03	7.949E-23	7.724E-23	2.722E-21	4.310E-22	4.414E-22	2.815E-23	3.243E-21	5.386E-22
	1.000E+04	7.192E-23	6.988E-23	2.610E-21	4.102E-22	4.244E-22	2.708E-23	3.106E-21	5.092E-22
	1.100E+04	6.556E-23	6.370E-23	2.520E-21	3.936E-22	4.097E-22	2.617E-23	2.995E-21	4.853E-22
	1.200E+04	5.976E-23	5.807E-23	2.430E-21	3.782E-22	3.958E-22	2.528E-23	2.886E-21	4.632E-22
23	5.130E+03	0.0	0.0	0.0	0.0	0.0	0.0	0.0	0.0
	5.165E+03	7.380E-23	6.775E-23	4.175E-22	1.382E-23	0.0	0.0	4.913E-22	8.157E-23
	5.190E+03	7.369E-23	6.765E-23	1.222E-21	2.081E-22	0.0	0.0	1.296E-21	2.758E-22
	5.250E+03	7.354E-23	6.751E-23	1.231E-21	2.149E-22	0.0	0.0	1.305E-21	2.824E-22
	5.500E+03	6.996E-23	6.422E-23	1.187E-21	1.993E-22	0.0	0.0	1.257E-21	2.635E-22
	6.035E+03	6.434E-23	5.906E-23	1.124E-21	1.741E-22	0.0	0.0	1.188E-21	2.332E-22
	6.070E+03	6.385E-23	5.861E-23	1.120E-21	1.728E-22	2.018E-22	6.673E-24	1.386E-21	2.381E-22
	6.100E+03	6.349E-23	5.828E-23	1.118E-21	1.717E-22	2.032E-22	6.736E-24	1.385E-21	2.367E-22
	6.250E+03	6.201E-23	5.693E-23	1.103E-21	1.661E-22	1.983E-22	6.613E-24	1.363E-21	2.296E-22
	6.500E+03	5.977E-23	5.487E-23	1.083E-21	1.579E-22	1.910E-22	6.432E-24	1.334E-21	2.192E-22
	7.500E+03	5.176E-23	4.752E-23	1.020E-21	1.335E-22	1.721E-22	5.985E-24	1.244E-21	1.870E-22
	8.500E+03	4.586E-23	4.210E-23	9.774E-22	1.180E-22	1.610E-22	5.727E-24	1.184E-21	1.658E-22
	1.000E+04	3.919E-23	3.598E-23	9.321E-22	1.034E-22	1.500E-22	5.457E-24	1.121E-21	1.448E-22
	1.210E+04	3.254E-23	2.987E-23	8.842E-22	9.140E-23	1.408E-22	5.213E-24	1.058E-21	1.265E-22
	1.400E+04	2.799E-23	2.569E-23	8.476E-22	8.443E-23	1.344E-22	5.018E-24	1.010E-21	1.151E-22
	1.600E+04	2.469E-23	2.267E-23	8.120E-22	7.893E-23	1.283E-22	4.817E-24	9.650E-22	1.064E-22
	1.800E+04	2.184E-23	2.005E-23	7.774E-22	7.441E-23	1.233E-22	4.643E-24	9.225E-22	9.910E-23
	2.000E+04	1.982E-23	1.819E-23	7.454E-22	7.060E-23	1.181E-22	4.460E-24	8.833E-22	9.325E-23
	2.200E+04	1.797E-23	1.650E-23	7.175E-22	6.747E-23	1.139E-22	4.305E-24	8.494E-22	8.828E-23
	2.400E+04	1.640E-23	1.506E-23	6.886E-22	6.443E-23	1.095E-22	4.143E-24	8.145E-22	8.363E-23
26	6.610E+03	0.0	0.0	0.0	0.0	0.0	0.0	0.0	0.0
	6.640E+03	4.451E-23	3.912E-23	2.529E-22	5.651E-24	0.0	0.0	2.974E-22	4.477E-23
	6.690E+03	4.459E-23	3.919E-23	7.477E-22	1.131E-22	0.0	0.0	7.923E-22	1.523E-22

TABLE VI. Excitation Autoionization Cross Sections for Li-like Ions

See page 309 for Explanation of Tables

Z	Ei	$Q_e(2s)$	$Q_{ea}(2s)$	$Q_e(2p)$	$Q_{ea}(2p)$	$Q_e(3p)$	$Q_{ea}(3p)$	Q_e	Q_{ea}
26	6.800E+03	4.418E-23	3.883E-23	7.449E-22	1.121E-22	0.0	0.0	7.891E-22	1.509E-22
	7.000E+03	4.315E-23	3.793E-23	7.275E-22	1.063E-22	0.0	0.0	7.706E-22	1.442E-22
	7.350E+03	4.113E-23	3.615E-23	7.051E-22	9.781E-23	0.0	0.0	7.462E-22	1.340E-22
	7.780E+03	3.890E-23	3.419E-23	6.833E-22	8.916E-23	0.0	0.0	7.222E-22	1.233E-22
	7.830E+03	3.859E-23	3.392E-23	6.813E-22	8.829E-23	1.232E-22	3.681E-24	8.431E-22	1.259E-22
	8.000E+03	3.767E-23	3.311E-23	6.742E-22	8.541E-23	1.217E-22	3.679E-24	8.336E-22	1.222E-22
	9.000E+03	3.372E-23	2.964E-23	6.381E-22	7.174E-23	1.096E-22	3.445E-24	7.814E-22	1.048E-22
	1.000E+04	3.042E-23	2.674E-23	6.129E-22	6.243E-23	1.020E-22	3.308E-24	7.453E-22	9.248E-23
	1.200E+04	2.531E-23	2.225E-23	5.796E-22	5.102E-23	9.276E-23	3.134E-24	6.977E-22	7.640E-23
	1.400E+04	2.178E-23	1.914E-23	5.551E-22	4.443E-23	8.718E-23	3.018E-24	6.641E-22	6.660E-23
	1.600E+04	1.919E-23	1.687E-23	5.334E-22	4.011E-23	8.326E-23	2.926E-24	6.359E-22	5.991E-23
	1.800E+04	1.696E-23	1.491E-23	5.151E-22	3.713E-23	8.001E-23	2.839E-24	6.121E-22	5.487E-23
	2.000E+04	1.538E-23	1.352E-23	4.973E-22	3.480E-23	7.708E-23	2.752E-24	5.898E-22	5.107E-23
	2.200E+04	1.391E-23	1.223E-23	4.818E-22	3.302E-23	7.458E-23	2.674E-24	5.703E-22	4.792E-23
	2.500E+04	1.229E-23	1.080E-23	4.575E-22	3.069E-23	7.093E-23	2.555E-24	5.407E-22	4.405E-23
	2.800E+04	1.100E-23	9.669E-24	4.375E-22	2.895E-23	6.783E-23	2.449E-24	5.163E-22	4.107E-23
	3.100E+04	9.871E-24	8.677E-24	4.171E-22	2.735E-23	6.480E-23	2.345E-24	4.918E-22	3.837E-23
29	8.280E+03	0.0	0.0	0.0	0.0	0.0	0.0	0.0	0.0
	8.325E+03	2.842E-23	2.364E-23	1.636E-22	2.579E-24	0.0	0.0	1.920E-22	2.622E-23
	8.380E+03	2.847E-23	2.368E-23	4.794E-22	6.584E-23	0.0	0.0	5.079E-22	8.953E-23
	8.450E+03	2.854E-23	2.374E-23	4.813E-22	6.623E-23	0.0	0.0	5.098E-22	8.997E-23
	8.800E+03	2.747E-23	2.285E-23	4.654E-22	6.123E-23	0.0	0.0	4.929E-22	8.408E-23
	9.760E+03	2.481E-23	2.064E-23	4.381E-22	5.031E-23	0.0	0.0	4.629E-22	7.095E-23
	9.810E+03	2.466E-23	2.051E-23	4.371E-22	4.985E-23	7.911E-23	2.272E-24	5.409E-22	7.264E-23
	9.900E+03	2.441E-23	2.031E-23	4.353E-22	4.904E-23	7.909E-23	2.266E-24	5.388E-22	7.161E-23
	1.050E+04	2.310E-23	1.922E-23	4.226E-22	4.412E-23	7.425E-23	2.172E-24	5.200E-22	6.551E-23
	1.200E+04	2.012E-23	1.674E-23	3.999E-22	3.526E-23	6.660E-23	2.037E-24	4.866E-22	5.404E-23
	1.400E+04	1.735E-23	1.443E-23	3.787E-22	2.801E-23	6.054E-23	1.929E-24	4.566E-22	4.438E-23
	1.600E+04	1.518E-23	1.263E-23	3.642E-22	2.361E-23	5.668E-23	1.855E-24	4.361E-22	3.809E-23
	1.800E+04	1.349E-23	1.122E-23	3.531E-22	2.076E-23	5.405E-23	1.802E-24	4.206E-22	3.378E-23
	2.000E+04	1.223E-23	1.017E-23	3.418E-22	1.871E-23	5.207E-23	1.757E-24	4.061E-22	3.065E-23
	2.200E+04	1.105E-23	9.192E-24	3.328E-22	1.726E-23	5.026E-23	1.711E-24	3.941E-22	2.816E-23
	2.500E+04	9.804E-24	8.156E-24	3.185E-22	1.560E-23	4.805E-23	1.650E-24	3.764E-22	2.541E-23
	2.800E+04	8.688E-24	7.228E-24	3.065E-22	1.444E-23	4.613E-23	1.593E-24	3.613E-22	2.326E-23
	3.100E+04	7.889E-24	6.563E-24	2.939E-22	1.348E-23	4.428E-23	1.535E-24	3.461E-22	2.158E-23
	3.400E+04	7.204E-24	5.993E-24	2.834E-22	1.275E-23	4.263E-23	1.481E-24	3.332E-22	2.022E-23
	3.800E+04	6.412E-24	5.334E-24	2.698E-22	1.192E-23	4.065E-23	1.416E-24	3.169E-22	1.867E-23

TABLE VII. Excitation Energies of the $1s2s^2$ State for Li-like Ions

See page 309 for Explanation of Tables

Z	$I_{ex}(2s)$	Z	$I_{ex}(2s)$	Z	$I_{ex}(2s)$
3	56.84	12	1320	21	4256
4	115.2	13	1563	22	4687
5	194.1	14	1827	23	5139
6	293.4	15	2111	24	5613
7	413.2	16	2416	25	6107
8	553.5	17	2742	26	6624
9	714.2	18	3089	27	7162
10	895.5	19	3457	28	7721
11	1097	20	3846	29	8303

TABLE VIII. Fit Parameters of Excitation Autoionization Cross Sections for Individual Ions

See page 309 for Explanation of Tables

Z	A (10^{-16}cm^2)	B
6	3.24	0.0082
8	2.65	0.0301
9	2.22	0.0547
12	1.20	0.285
13	0.956	0.462
14	0.773	0.663
17	0.475	1.18
23	0.254	2.26
26	0.146	3.91
29	0.0621	9.19